
COMPARISON OF CATALOGS

A PREPRINT

September 30, 2024

Table of contents

1	The data	1
2	Catalog Completeness	2
2.1	Completeness of the LCV Catalog	2
2.2	Completeness of HECATE	3
2.3	Completeness of the Inner join	3
2.4	Completeness in Outer join	3
2.5	Completeness of the Data	3
2.5.1	Distance	3
3	How are we going to compare the data?	4
3.1	Scatter plots and R^2 calculation	4
4	Comparable data	5
4.1	Coordinates	5
4.1.1	Right Ascension	5
4.1.2	Declination	6
4.1.3	Distance	6
4.2	Velocities	6
4.3	Morphology and Geometry	8
4.3.1	Galaxy Types	9
4.3.2	Inclination	10
4.3.3	Major Axis	11
4.4	Luminosities	11
4.5	Magnitudes	12
4.5.1	B mag	13
4.5.2	K mag	13
4.6	SFR	14
4.7	Masses	15
4.7.1	Stellar Masses Comparison	16
4.7.2	Heatmap	17

1 The data

In this script we will compare 2 catalogs Kovlakas et al. (2021) and Karachentsev and Kaisina (2013)

- The data have been joined based on their position in the sky (Ra, Dec).
 - We assume that every galaxy within 2 arc seconds of the initial coordinates is the same galaxy.
- We use TOPCAT to create two joins, an inner and an outer join
- We will use the inner join for 1-1 comparisons
- If we see that the data are similar we can use the outer join

- For the comparison we keep the parameters names exactly they are given in the catalogs

The dataset we are going to use for the comparison (inner join) consists of 288 galaxies and 168 columns.

2 Catalog Completeness

Checking for completeness in galaxy catalogs is essential to ensure that the data accurately represents the true population of galaxies. Incomplete catalogs can lead to biased results in statistical studies, such as the distribution of galaxy luminosity, mass, or star formation rates. Additionally, missing galaxies, especially those at faint magnitudes or large distances, can distort cosmological measurements and hinder our understanding of galaxy formation and evolution.

Completeness checks are crucial for addressing selection biases, identify gaps in the data and guide follow-up observations, ensuring that the catalog provides a reliable sample for scientific analysis. Without these checks, conclusions drawn from the data may be inaccurate or incomplete.

2.1 Completeness of the LCV Catalog

The local volume selection has been made by taking into account galaxies with: 1. Radial velocities of

$$V_{LG} < 600 \text{ km} \cdot \text{s}^{-1} \quad (1)$$

2. Distances of $D < 11 \text{ Mpc}$

A simultaneous fulfillment of both conditions (1) and (2) is not required.

- Completeness within a 10 Mpc radius is difficult to assess due to:
 - Variability in galaxy properties (luminosity, size, surface brightness, gas content)
 - Errors in distance measurements (Tully–Fisher method errors of ~20–25%), especially at the 10 Mpc boundary.
 - * Accurate distances are mainly known within ~5 Mpc.
 - Non-Hubble motions (~300 km/s) may make up half of the adopted velocity constraint Equation 1
 - * Solution for our usage: only keep the galaxies inside a radius of $D = 11 \text{ Mpc}$
 - * HI sources in surveys with low angular resolution: “The presence around our Galaxy of hundreds of high-velocity clouds with low line-of-sight velocities and small W50 widths also provokes the inclusion of false “nearby” dwarf galaxies in the LV” Karachentsev, Makarov, and Kaisina (2013)
 - * photographic emulsion defect -> exotic cases of galaxies -> radial velocity of $+614 \text{ km s}^{-1}$
- Astro-Spam and Survey Errors:
 - Automatic surveys produce false detections (e.g., stars misclassified as galaxies, high-velocity clouds mistaken for dwarfs).
- Conditional Completeness Estimate:
 - Galaxies brighter than $M_B^c = -11^m$ or with linear diameters larger than $A_{26} = 1.0 \text{ kpc}$ show (40–60)% completeness.
 - “among the members of the Local Group ($D < 1 \text{ Mpc}$), only half of the galaxies have absolute magnitudes brighter than 11m. Consequently, more than half of the ultra-faint dwarf companions around normal galaxies, like the Sombrero galaxy ($D = 9.3 \text{ Mpc}$), still remain outside our field of view.”
- Undetected Ultra-Faint Dwarfs:
 - Many faint dwarf galaxies remain undetected beyond the Local Group. Estimated population of undetected dwarfs could be as large as 10^3 – 10^4 within the LV.
- Surface Brightness Distribution:
 - Surface brightness remains consistent across distances, except for ultra-faint dwarfs ($SB < 31 \text{ mag} \cdot \text{arcsec}^{-2}$).
 - Faintest dwarf galaxies are detectable only nearby due to their resolution into individual stars.
- Luminosity-Size Relationship:
 - Observations align with cosmological models predicting $L \sim A^3$ Navarro, Frenk, and White (1996), though deviations occur for extremely low surface brightness galaxies.
 - “The deviation from it at the extremely low surface brightness end is due to a systematic overestimation of dwarf galaxy sizes, the brightness profiles of which lie entirely below the Holmberg isophote.”

2.2 Completeness of HECATE

The completeness of HECATE is difficult to assess due to: - Unknown selection function of HyperLEDA and selection effects from other cross-correlated catalogs. - Estimation based on comparing B-band luminosity distribution with the galaxy luminosity function (LF).

- HECATE is:
 - Complete down to $L_B \sim 10^{9.5} L_{B,\odot}$ for distances less than 33 Mpc.
 - Complete down to $L_B \sim 10^{10} L_{B,\odot}$ for distances between 67 Mpc and 100 Mpc.
 - Incomplete at distances greater than 167 Mpc, even for the brightest galaxies.
- Completeness estimates based on B-band luminosity density:
 - >75% complete for distances less than 100 Mpc. $\sim 50\%$ complete at distances of ~ 170 Mpc.
 - Completeness exceeds 100% within 30 Mpc due to the overdensity of galaxies around the Milky Way.
- Completeness in terms of stellar mass (M^*):
 - Similar to B-band completeness when measured with K_s-band luminosity as a tracer for stellar mass. Overdensity at small distances and cut-off at large distances are observed.
- Completeness in terms of star formation rate (SFR):
 - $\sim 50\%$ complete between 30 and 150 Mpc.
 - Lower SFR completeness due to limitations in WISE-based SFR estimates, which lack full sky coverage.
 - Despite IRAS's limited depth, it provides >50% coverage for star-forming galaxies in the local neighborhood.

In this section we will check the completeness

Table	Number of galaxies
Inner join	288
Outer join	2901
LCV	1316
HECATE	2901
Unique galaxies in LCV	1028
Unique Galaxies in Hecate	2613

2.3 Completeness of the Inner join

$$\text{Completeness (X)} = \frac{(\text{Galaxies in Inner Join})}{(\text{Galaxies in X})} \times 100\%$$

Completeness (HECATE)= 10 %

Completeness (LCV)= 22 %

2.4 Completeness in Outer join

$$\text{Completeness (X)} = \frac{(\text{Galaxies in Outer Join form X})}{(\text{Galaxies in X})} \times 100\%$$

Completeness (HECATE)= 90 %

Completeness (LCV)= 78 %

$$\text{Combined Completeness} = \frac{\text{Total galaxies in Outer}}{\text{Unique galaxies in HECATE + LCV}} = 80 \%$$

2.5 Completeness of the Data

2.5.1 Distance

As we can see from the histograms Figure 1 and Figure 2 the sample of unique galaxies of each catalog, gets smaller by an almost constant proportion (Inner join).

This means there is no bias in the selection of the galaxies.

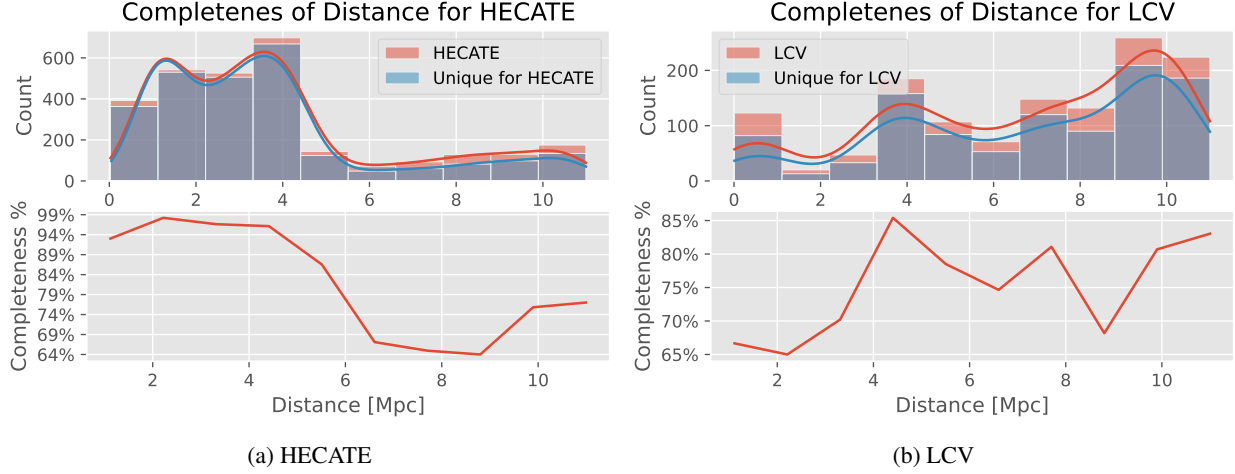


Figure 1: Histograms showing the Distance Completeness of the Catalogs

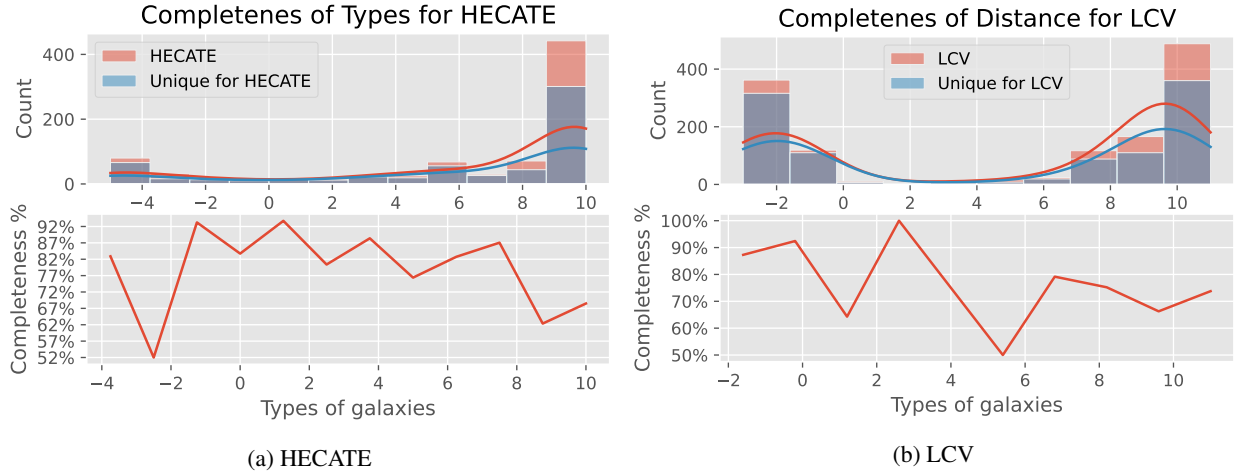


Figure 2: Histograms showing the Type Completeness of the Catalogs

3 How are we going to compare the data?

3.1 Scatter plots and R^2 calculation

1. R^2 : Measures the proportion of variance explained by the linear model.
 2. Slope of the Fitted Line: Should be close to 1 for a 1-1 correlation.¹
 3. Pearson Correlation ρ : Measures the strength and direction of the linear relationship between two variables, ranging from -1 to 1.²
 4. Plots: Plots are essential for visually assessing the relationship between two datasets, identifying correlations, trends, and outliers, and evaluating the fit of linear models.
- Histograms: Because not all of our data have the same number of counts, the comparison with histograms between data that are not the same, doesn't help us right now.³ This is why we will only use histograms for comparing the distribution of same-data columns normalized by their maximum value

¹Some data seem to have a very good linear correlation but they have many outliers. This is why we will clip the outliers with $\sigma > 3$

²In simple linear regression, R^2 is the square of the Pearson correlation coefficient ρ .

³When we will use the outer join table we could use histograms due to the large number of counts.

- **Correlation Heatmaps:** A correlation heatmap is a graphical tool that displays the correlation between multiple variables as a color-coded matrix. It's like a color chart that shows us how closely related different variables are. In a correlation heatmap, each variable is represented by a row and a column, and the cells show the correlation between them. The color of each cell represents the strength and direction of the correlation, with darker colors indicating stronger correlations.
 - **Kernel Density Estimate (KDE) plot:** The KDE plot visually represents the distribution of data, providing insights into its shape, central tendency, and spread.
5. **Percentage change:** We can calculate the percentage change of the data for each galaxy and then we can see if the data are similar, based on minimum, the maximum and the mean value of the difference.

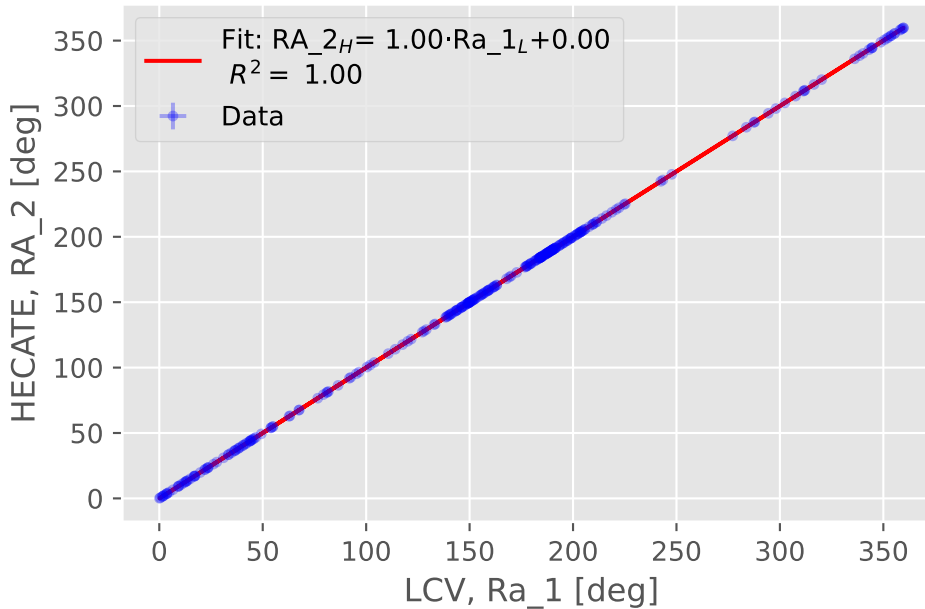
$$\text{Percentage change} = \frac{V_{Hecate} - V_{LCV}}{V_{Hecate}} \cdot 100\%$$

4 Comparable data

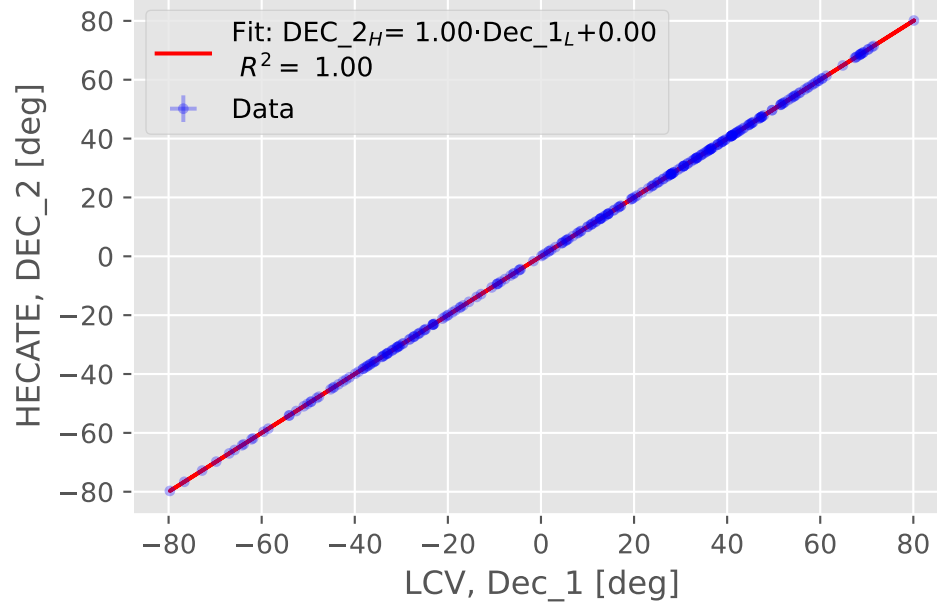
4.1 Coordinates

LCV	HECATE	Description	Pearson Correlation [-1,1]
Ra_1	RA_2	Right Ascension	1.0
Dec_1	DEC_2	Declination	1.0
Dis	D	Distance	0.881

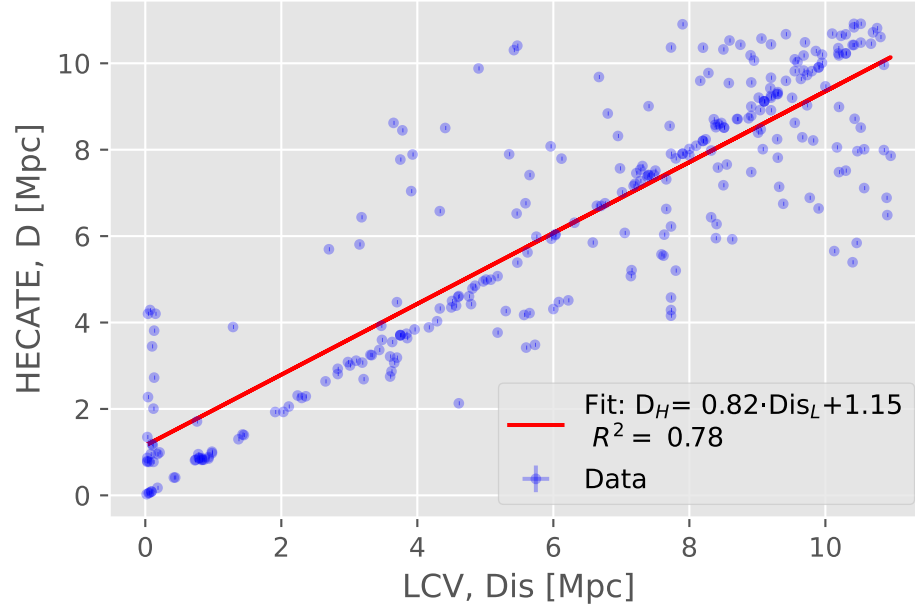
4.1.1 Right Ascension



4.1.2 Declination

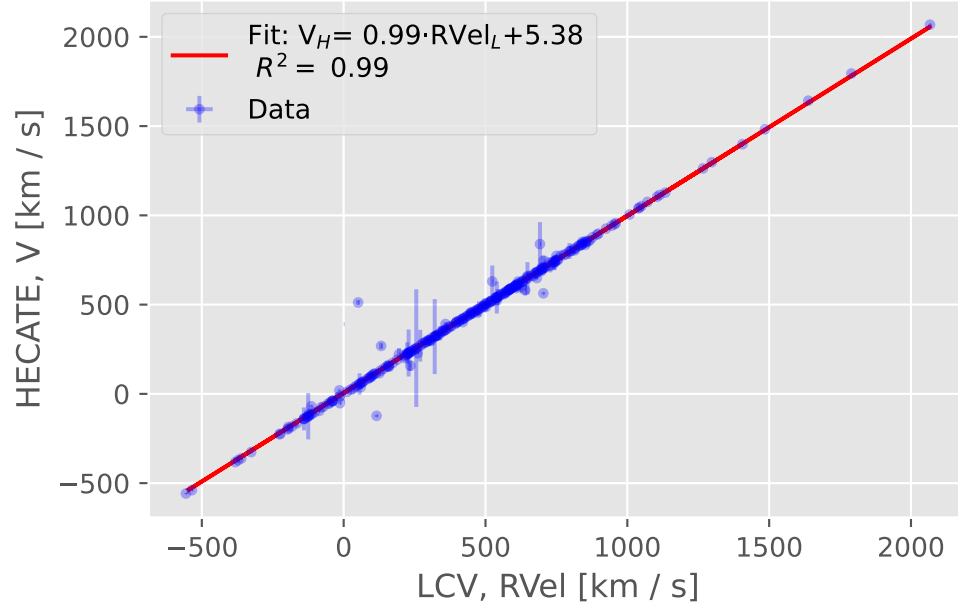


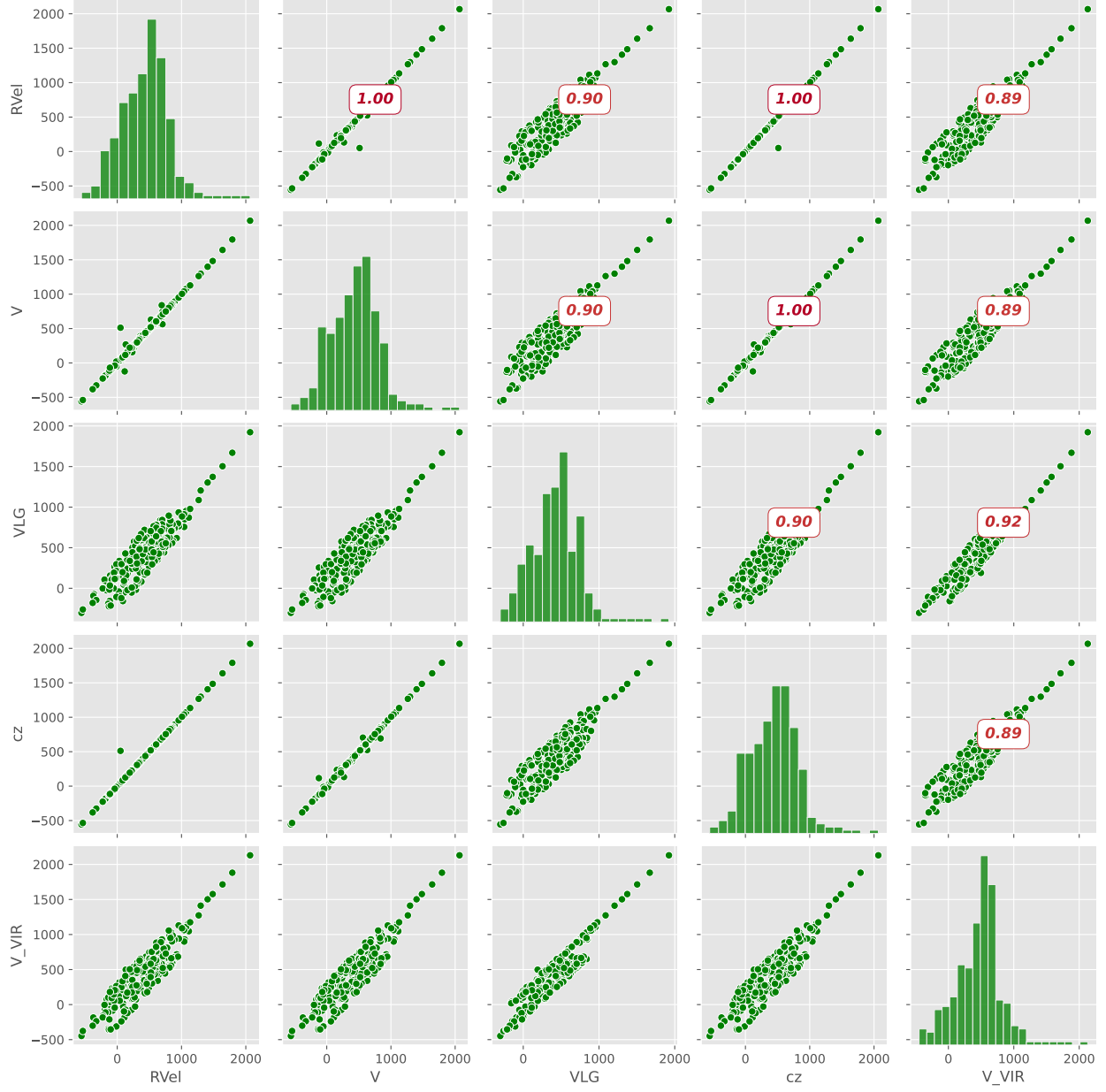
4.1.3 Distance



4.2 Velocities

LCV	HECATE	Description	Linear Correlation
RVel (km/s)	V (km/s)	Heliocentric radial velocity	0.994
VLG (km/s)		Radial velocity	
cz (km/s)		Heliocentric velocity	
	V_VIR (km/s)	Virgo-infall corrected radial velocity	



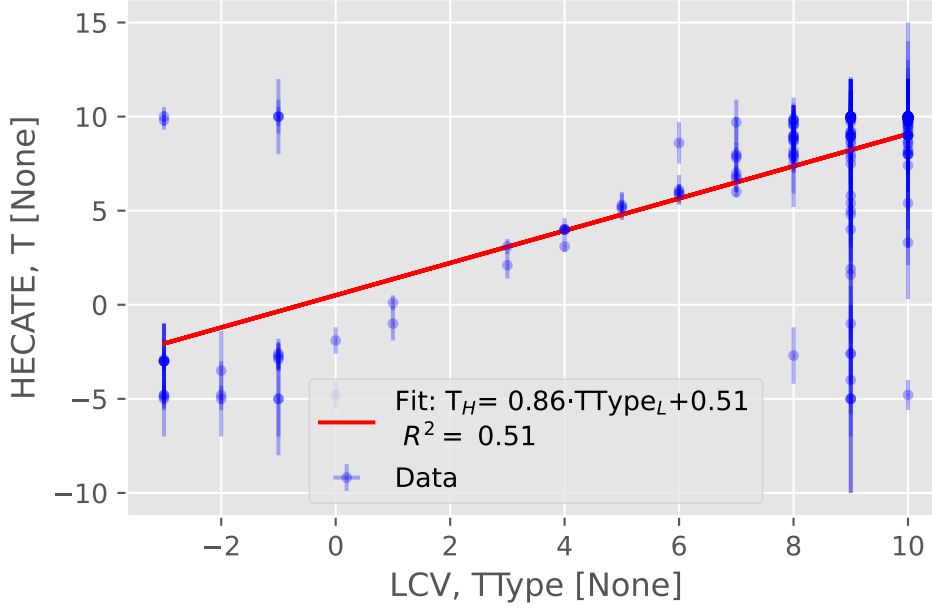


[?] The close correlation between all of the velocities, could be due to the fact that all of them measure the velocity of each galaxy, but from a different frame of reference.

4.3 Morphology and Geometry

LCV	HECATE	Description	Pearson Correlation [-1,1]
TType	T (with errors)	Numerical Hubble type following the de Vaucouleurs system	0.7107
inc	INCL	Inclination (deg)	0
a26_1 (Major)	R1 (Semi-major axis)	angular diameter (arcmin)	0

4.3.1 Galaxy Types

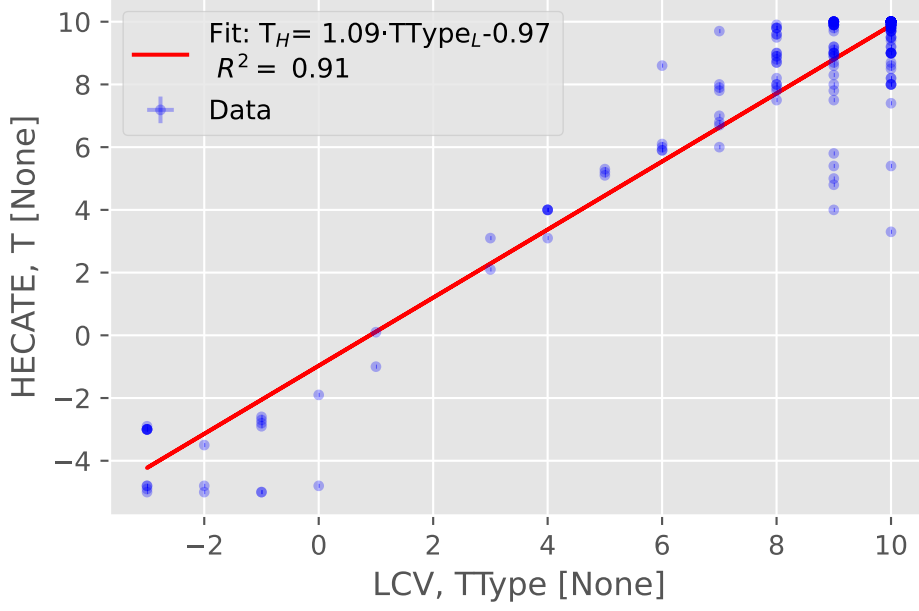


“Morphological type of galaxy in the numerical code according to the classification by de Vaucouleurs et al. (1991). It should be noted that about three quarters of objects in the LV are dwarf galaxies, which require a more detailed morphological classification. For example, dwarf spheroidal galaxies and normal ellipticals are usually denoted by the same numerical code $T < 0$, although their physical properties drastically differ. The classification problem arises as well for the “transient” type dwarf galaxies, T_r , which combine the features of spheroidal (Sph) and irregular (Ir) systems. Due to small classification errors, such objects may “jump” from one end of the T scale to the other.” Karachentsev, Makarov, and Kaisina (2013)

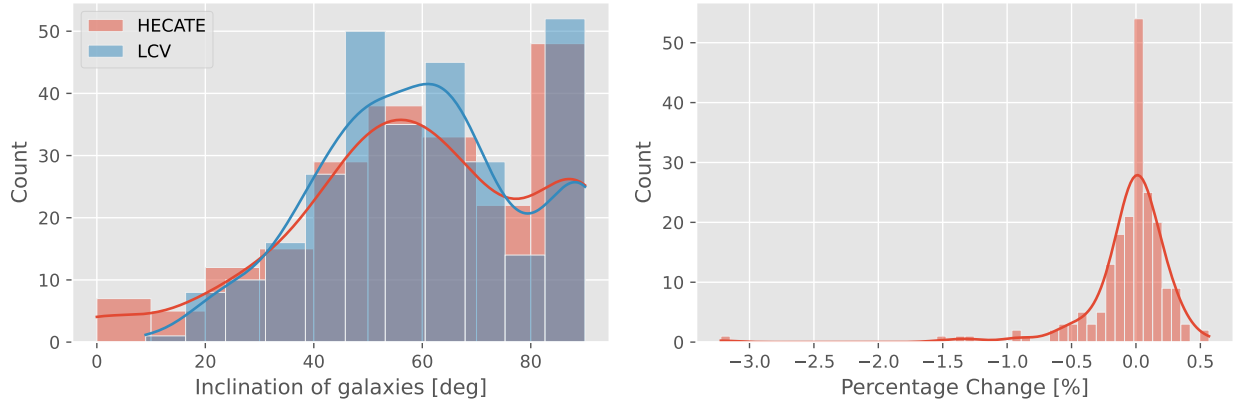
- we can assume that the galaxies from the upper left and lower right regions of the plot are classified differently because of this
- this might explain the large errors E_T of HECATE
- why we see a difference in the distribution of Figure 2

We can remove the “problematic” galaxies by only keeping the ones with:

$$|T_{HECATE} - T_{LCV}| < 7$$



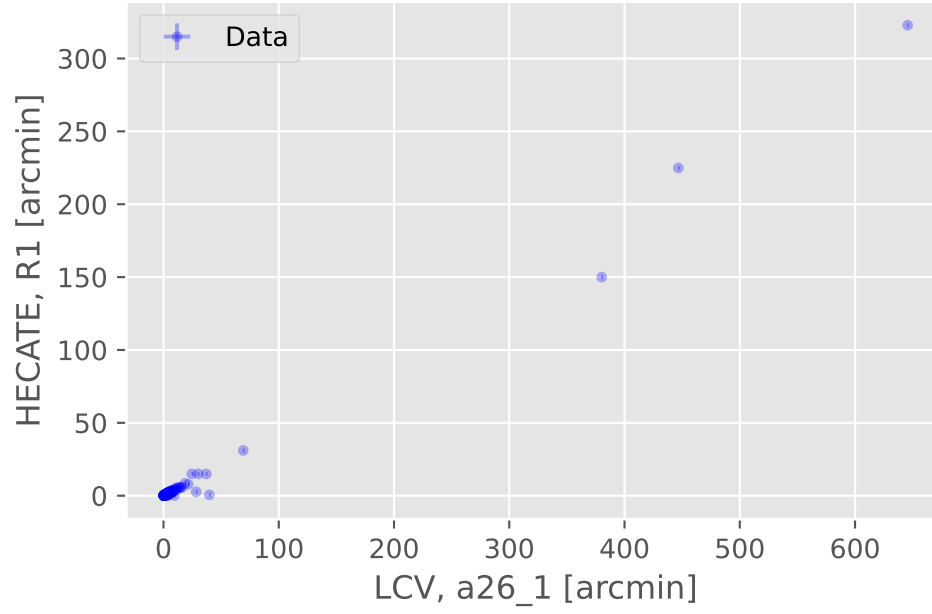
4.3.2 Inclination



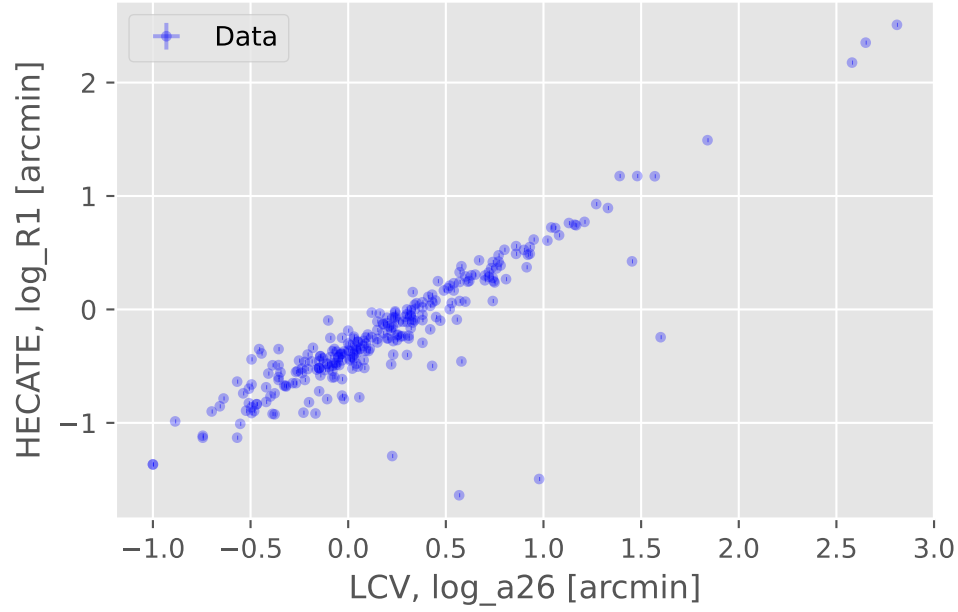
	inc	INCL	Percentage Change [%]
count	287	209	202
mean	60	59	-0
std	19	23	0
min	9	0	-3
25%	47	47	-0
50%	60	59	0
75%	72	78	0
max	90	90	1

We can see that for values in the range $[\sim 30^\circ, \sim 80^\circ]$, the values of the LCV inclination are higher. However, since their means, median, min and maxes are similar and the percentage change is practically 0% (mean, median, $\sigma = 0$ with a range $[-3\%, 1\%]$), we can ignore the differences and assume they are the same values.

4.3.3 Major Axis

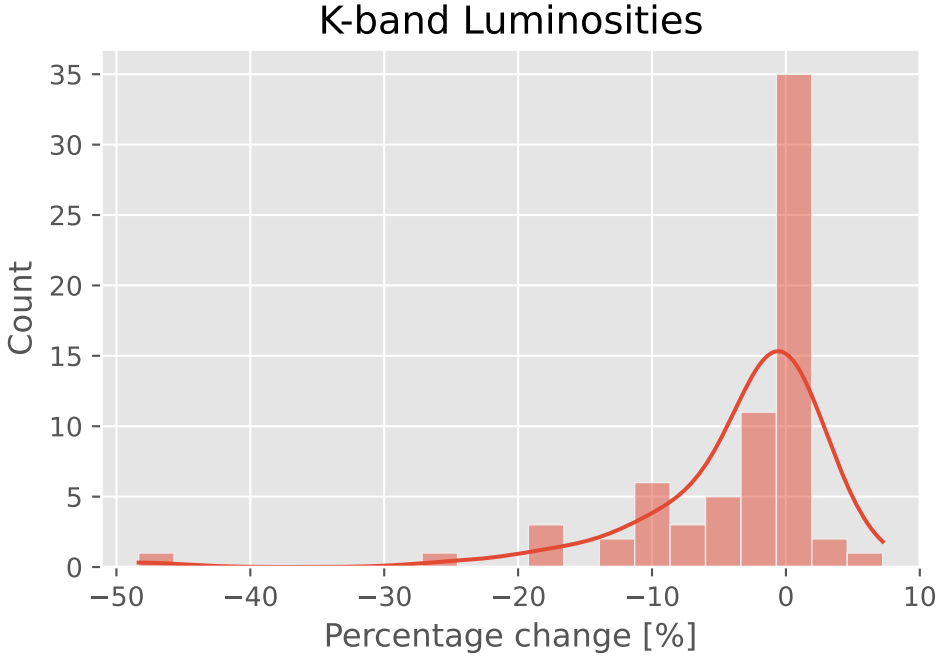


it is not very clear if we truly have a correlation or not. We need to see the linear correlation of the decimal logarithms.



4.4 Luminosities

LCV	HECATE	Description	Pearson Correlation [-1,1]
logKLum	logL_K		0

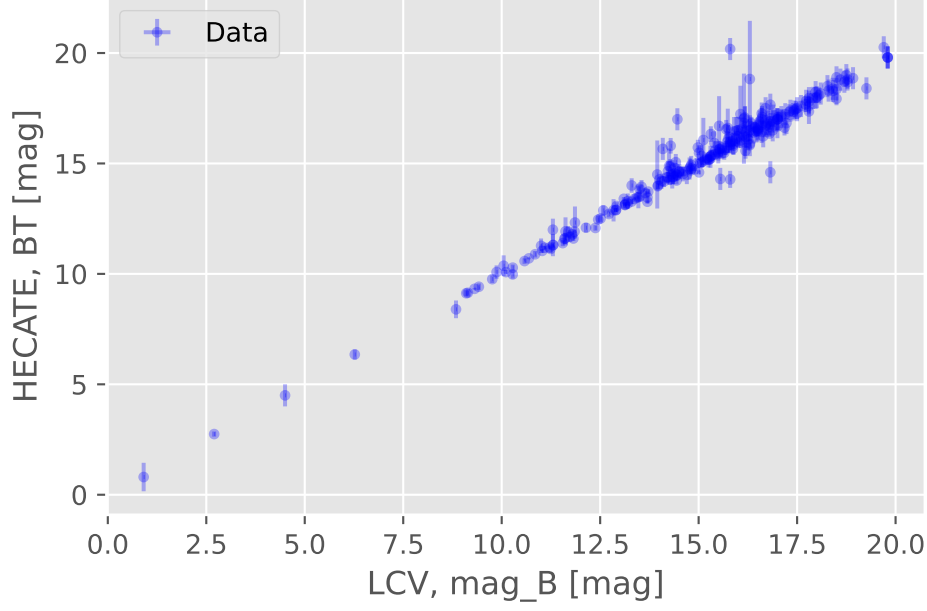


	$\log(L_K)_{\{LCV\}}$	$\log(L_K)_{\{HEC\}}$	Percentage Change [%]
count	287	70	70
mean	8	9	-4
std	1	1	8
min	3	5	-48
50%	8	9	-0
max	11	11	7

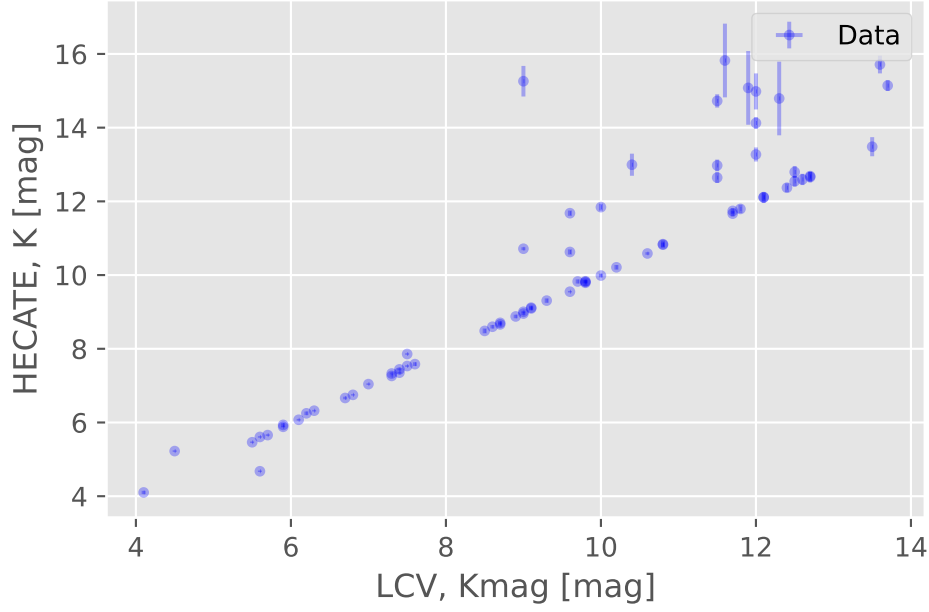
4.5 Magnitudes

LCV	HECATE	Description	Pearson Correlation [-1,1]
mag_B (with errors)	BT (with errors)		0
Kmag	K	2MASS band magnitude (both)	0

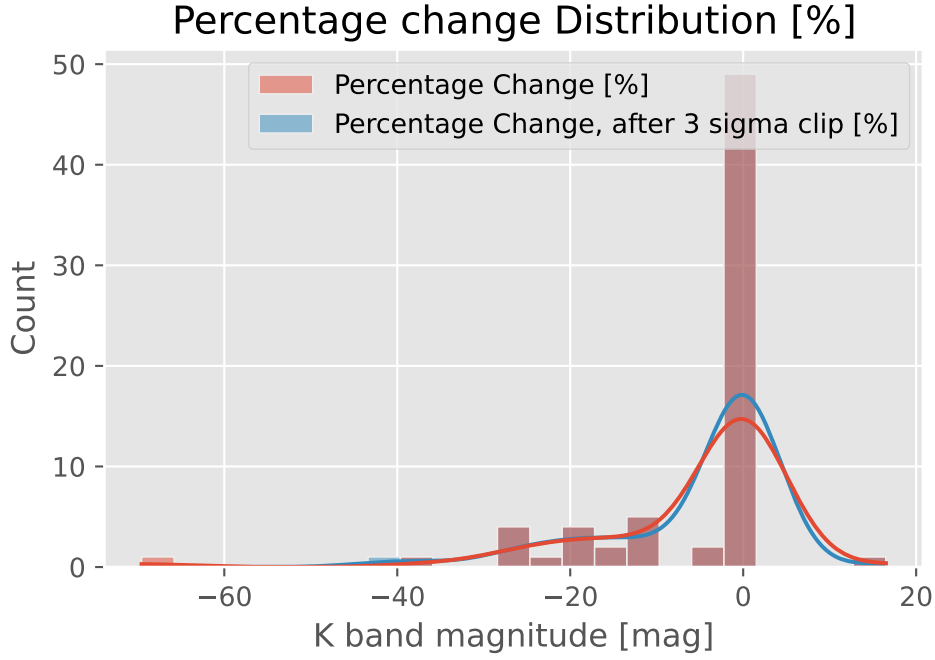
4.5.1 B mag



4.5.2 K mag



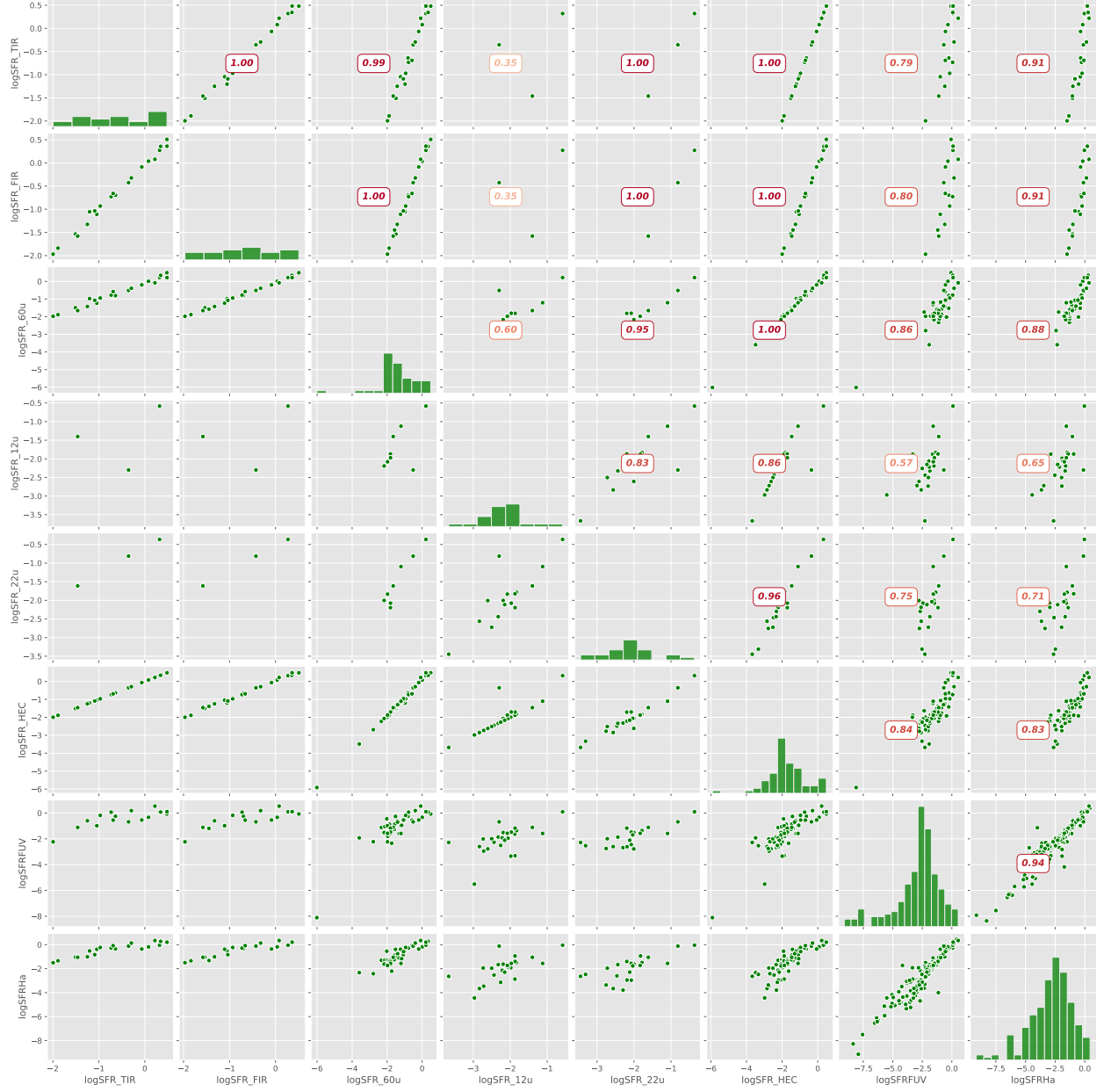
	Percentage Change [%]	Percentage Change, after 3 sigma clip [%]
count	70	70
mean	-5	-5
std	12	10
min	-70	-42
50%	-0	-0
max	16	16



[?]

4.6 SFR

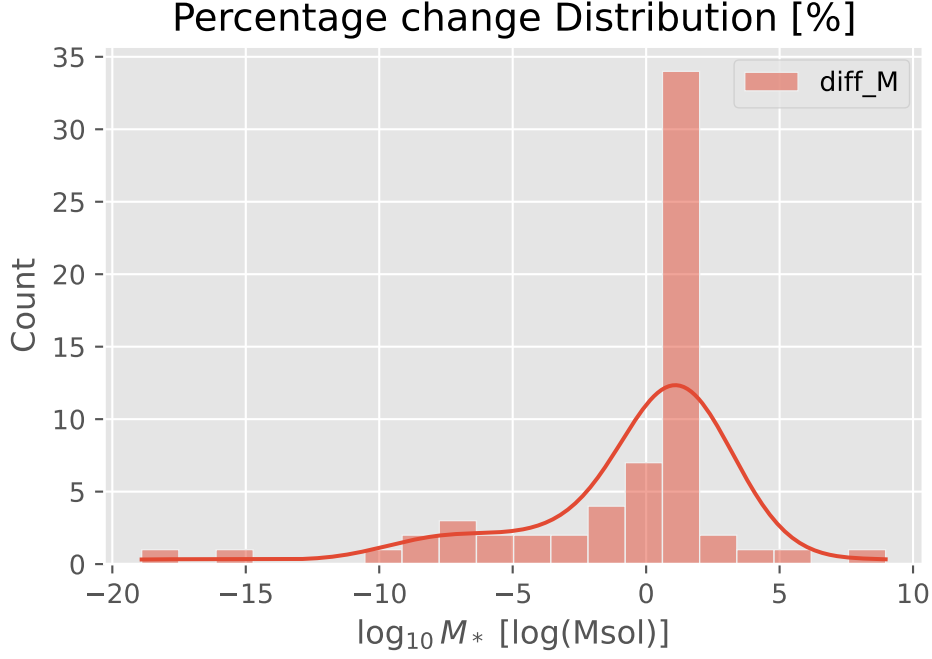
LCV	HECATE	Description	Count
	logSFR_TIR	Decimal logarithm of the total-infrared SFR estimate [Msol/yr]	21
	logSFR_FIR	Decimal logarithm of the far-infrared SFR estimate [Msol/yr]	22
	logSFR_60u	Decimal logarithm of the 60um SFR estimate [Msol/yr]	48
	logSFR_12u	Decimal logarithm of the 12um SFR estimate [Msol/yr]	26
	logSFR_22u	Decimal logarithm of the 22um SFR estimate [Msol/yr]	23
	logSFR_HEC	Decimal logarithm of the homogenised SFR estimate [Msol/yr]	73
	logSFR_GSW	Decimal logarithm of the SFR in GSWLC-2 [Msol/yr]	0
SFRFUV		FUV derived integral star formation rate	220
SFRHa		H{alpha} derived integral star formation rate	223



4.7 Masses

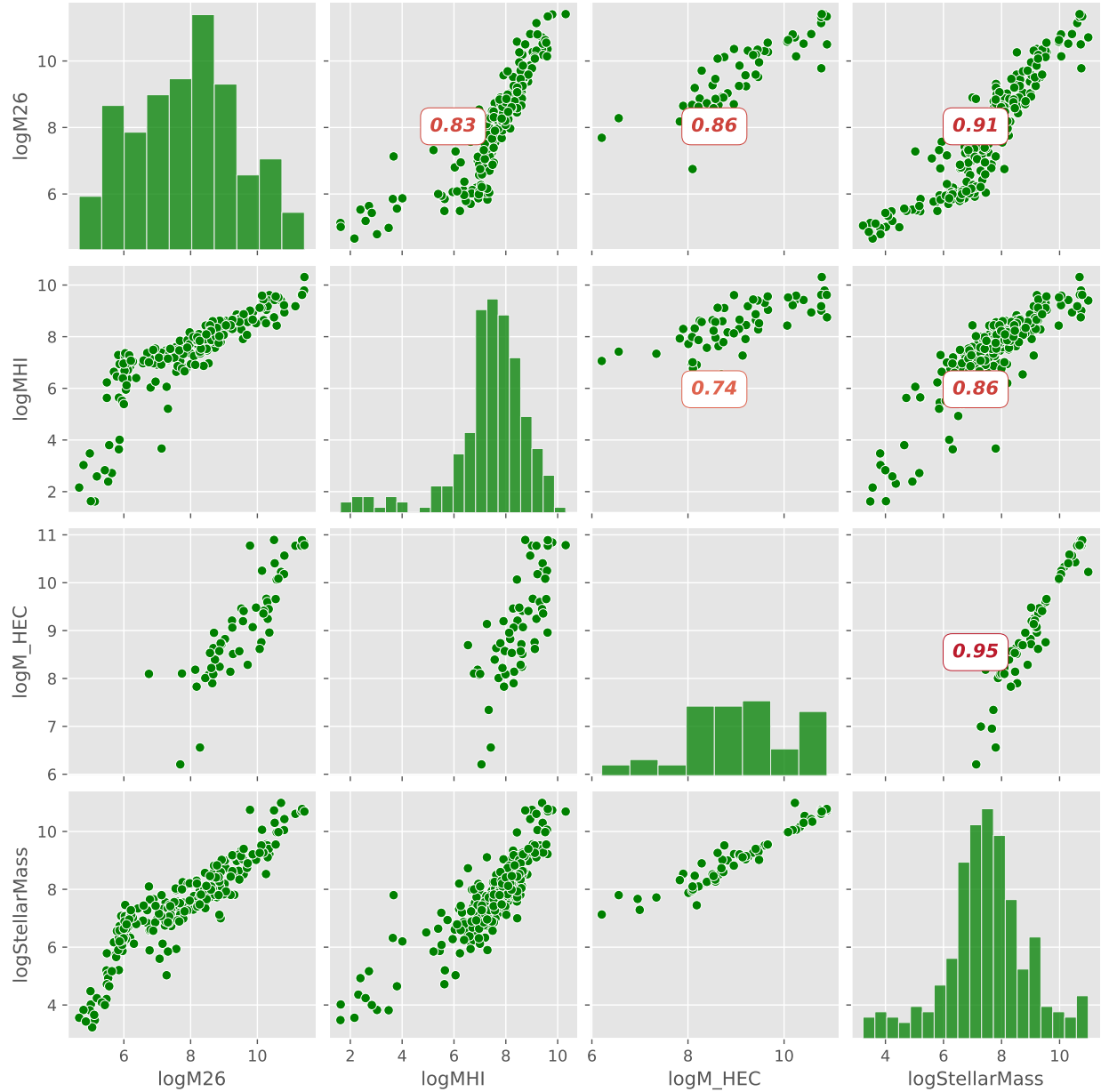
LCV	HECATE	Description	Count
logM26		Log mass within Holmberg radius	233
logMHI		Log mass within Holmberg radius	233
	logM_HEC	Decimal logarithm of the stellar mass [Msol]	64
	logM_GSW	Decimal logarithm of the stellar mass in GSWLC-2 [Msol]	0
logStellarMass		Stellar Mass from $M_*/L = 0.6$	287

4.7.1 Stellar Masses Comparison



	Percentage Change [%]
count	64
mean	-1
std	5
min	-19
50%	1
max	9

4.7.2 Heatmap



Karachentsev, Igor D., and Elena I. Kaisina. 2013. “STAR FORMATION PROPERTIES IN THE LOCAL VOLUME GALAXIES VIA H AND FAR-ULTRAVIOLET FLUXES.” *The Astronomical Journal* 146 (3): 46. <https://doi.org/10.1088/0004-6256/146/3/46>.

Karachentsev, Igor D., Dmitry I. Makarov, and Elena I. Kaisina. 2013. “UPDATED NEARBY GALAXY CATALOG.” *The Astronomical Journal* 145 (4): 101. <https://doi.org/10.1088/0004-6256/145/4/101>.

Kovlakas, K., A. Zezas, J. J. Andrews, A. Basu-Zych, T. Fragos, A. Hornschemeier, K. Kouroumpatzakis, B. Lehmer, and A. Ptak. 2021. “The Heraklion Extragalactic Catalogue (HECATE): A Value-Added Galaxy Catalogue for Multimessenger Astrophysics.” *Monthly Notices of the Royal Astronomical Society* 506 (September): 1896–1915. <https://doi.org/10.1093/mnras/stab1799>.

Navarro, Julio F., Carlos S. Frenk, and Simon D. M. White. 1996. “The Structure of Cold Dark Matter Halos.” *The Astrophysical Journal* 462 (May): 563. <https://doi.org/10.1086/177173>.